



Cupriavidus metallidurans NA4 actively forms polyhydroxybutyrate-associated uranium-phosphate precipitates

Tom Rogiers^{a,b}, Mohamed L. Merroun^c, Adam Williamson^{b,1}, Natalie Leys^a, Rob Van Houdt^a, Nico Boon^b, Kristel Mijndonckx^{a,*}

^a Microbiology Unit, Interdisciplinary Biosciences, Belgian Nuclear Research Centre, SCK CEN, Mol, Belgium

^b Center for Microbial Ecology and Technology (CMET), UGent, Ghent, Belgium

^c Department of Microbiology, University of Granada, Granada, Spain

ARTICLE INFO

Editor: Dr. R. Deborá

Keywords:

C. metallidurans
Uranium
PHB
Transcriptomics
Metal resistance

ABSTRACT

Cupriavidus metallidurans is a model bacterium to study molecular metal resistance mechanisms and its use for the bioremediation of several metals has been shown. However, its mechanisms for radionuclide resistance are unexplored. We investigated the interaction with uranium and associated cellular response to uranium for *Cupriavidus metallidurans* NA4. Strain NA4 actively captured $98 \pm 1\%$ of the uranium in its biomass after growing 24 h in the presence of 100 μM uranyl nitrate. TEM HAADF-EDX microscopy confirmed intracellular uranium-phosphate precipitates that were mainly associated with polyhydroxybutyrate. Furthermore, whole transcriptome sequencing indicated a complex transcriptional response with upregulation of genes encoding general stress-related proteins and several genes involved in metal resistance. More in particular, gene clusters known to be involved in copper and silver resistance were differentially expressed. This study provides further insights into bacterial interactions with and their response to uranium. Our results could be promising for uranium bioremediation purposes with the multi-metal resistant bacterium *C. metallidurans* NA4.

1. Introduction

Anthropogenic activities like ore mining and processing, phosphate mining for fertilizer production, and oil and gas production, contribute to an increase in naturally occurring radioactive materials (NORM) such as uranium (IAEA, 2003; Ma et al., 2020; Rogiers et al., 2021). Consequently, these activities result in a reoccurring contamination of uranium in soil and groundwater, which poses a threat when accumulated through the food chain [Reviewed in 2]. The severity of this bioaccumulation depends on the mobility of uranium.

Microorganisms can influence the mobility of uranium through biosorption (Francis et al., 2004), redox transformations (Suzuki et al., 2005; Beller, 2005), uptake and intracellular accumulation (Suzuki and Banfield, 2004), and biomineralization with phosphates (Jroundi et al., 2007; Martinez et al., 2007) and carbonates (Carvajal et al., 2012; Merroun and Selenska-Pobell, 2008). In turn, uranium exerts pressure on the microbial community and can change its structure and functional properties (Lopez-Fernandez et al., 2018; Sutcliffe et al., 2017).

Investigating the interaction between microorganisms and uranium is important to correctly assess the behavior of uranium in contaminated environments. Most studies focus on the phenotypical interaction between microorganisms and uranium while the cellular response could provide additional insights on molecular resistance mechanisms and the toxic effect of uranium. Although a shift has been made in the last two decades, detailed understanding on the molecular mechanisms is still lacking. Nevertheless, comprehensive insights in these mechanisms are necessary for the development and optimization of uranium biosensors and can aid bioremediation processes (Hillson et al., 2007). Phosphatase activity have been shown to be involved in extra- and intracellular uranium-phosphate precipitation in several strains e.g. *Citrobacter* (Macaskie et al., 2000), *Bacillus* (Beazley et al., 2007), *Sphingomonas* (Merroun et al., 2011), *Caulobacter crescentus* (Hu et al., 2005; Yung and Jiao, 2014) and *Stenotrophomonas bentonitica* BII-R7 (Pinel-Cabello et al., 2021). Moreover, several genes have been identified that play a key role in uranium resistance in *Caulobacter crescentus* (Yung et al., 2015). These genes comprise two outer membrane transporters, a

* Corresponding author.

E-mail addresses: tom.rogiers@sckcen.be (T. Rogiers), merroun@ugr.es (M.L. Merroun), adjwilliamson@gmail.com (A. Williamson), natalie.leys@sckcen.be (N. Leys), rob.van.houdt@sckcen.be (R.V. Houdt), nico.boon@ugent.be (N. Boon), kmijnend@sckcen.be (K. Mijndonckx).

¹ Current address: Centre Etudes Nucléaires de Bordeaux Gradignan, CENBG, Bordeaux, France.

<https://doi.org/10.1016/j.jhazmat.2021.126737>

Received 9 April 2021; Received in revised form 21 July 2021; Accepted 22 July 2021

Available online 30 July 2021

0304-3894/© 2021 The Authors. Published by Elsevier B.V. This is an open access article under the CC BY license (<http://creativecommons.org/licenses/by/4.0/>).

stress-responsive transcription factor, and a ppGpp synthetase/hydrolase in the absence of glucose (Yung et al., 2015). Proteins involved in phosphate and iron metabolic pathways were induced in *Microbacterium oleivoras* A9 after uranium exposure. However, the link between iron metabolism and uranium resistance remains unclear (Gallos et al., 2018; Theodorakopoulos et al., 2015). In anoxic environments, c-type cytochromes are important in the reduction of bioavailable U^{6+} to water insoluble U^{4+} in *Geobacter* and *Shewanella* species (Holmes et al., 2009; Anderson et al., 2003; Shelobolina et al., 2007, 2008; Shi et al., 2011; Ghasemi et al., 2020; Ganesh et al., 1997), and uranium removal capacity was reduced when genes involved in nitrogen metabolism and oxidative phosphorylation were introduced in *Bacillus atrophaeus* ATCC 9372 (Wang et al., 2019).

The model bacterium *C. metallidurans* is known to harbor a wide plethora of metal resistance genes and strains are typically isolated from metal-contaminated environments (Diels and Mergeay, 1990; Mijnen-donckx et al., 2013). Moreover, strain *C. metallidurans* NA4 has been shown to be able to adapt to toxic metal concentrations and its genome has been completely resolved (Ali et al., 2019; Mijnen-donckx et al., 2019). However, its radionuclide resistance mechanisms are largely unknown. Here, we studied the interaction of *C. metallidurans* strain NA4 with uranium. To this end, the strain was grown in the presence of uranyl nitrate and removal was measured and analyzed with Inductively Coupled Plasma-Mass Spectrometry (ICP-MS) and high-angle annular dark-field scanning transmission electron microscopy combined with Energy-dispersive X-ray spectroscopy (STEM HAADF-EDX), respectively. In addition, its response to uranium was revealed by whole transcriptome profiling.

2. Materials and methods

2.1. Strains, media and culture conditions

C. metallidurans NA4 was routinely cultured in RM medium (Mergeay et al., 1985) with a final composition of 4.68 g/L NaCl, 1.49 g/L KCl, 1.07 g/L NH_4Cl , 0.43 g/L Na_2SO_4 , 0.2 g/L $MgCl_2 \cdot 6H_2O$, 0.03 g/L $CaCl_2 \cdot 2H_2O$, 0.02 mM $Fe(NH_4)$ citrate, 20 mM MOPS buffer (pH 7 stock), 0.95 mM $Na_2\beta$ -glycerol phosphate and 1 mL of the trace element solution SL7 of Biebl and Pfennig (Biebl and Pfennig, 1981). RM was supplemented with 0.2% (wt/vol) sodium gluconate as a carbon source. Cultures were grown in the dark at 30 °C with shaking at 120 rpm. For culturing on solid media, 2% agar (bacteriological, OXOID, United Kingdom) was added. Uranium was added as $UO_2(NO_3)_2 \cdot 6H_2O$ (dissolved in 100 mM HCl, SPI chemicals, USA).

2.2. Uranium resistance of *C. metallidurans* NA4

Three independent stationary phase cultures grown in RM medium for two days were pelleted for 5 min at 8500 g, washed with 10 mM $MgSO_4$ and diluted to a cell concentration of 1×10^7 cells/mL in a flat bottom 96-well plate (Cellstar 96 Well Cell Culture Plate, Greiner Bio-One, Belgium) that contained RM medium with or without different $UO_2(NO_3)_2$ concentrations. Growth (OD_{595}) was monitored for three days at 30 °C, 300 rpm in a 96-well plate reader (Multiskan Ascent, Thermo LabSystems). Growth curves were analyzed with the R Growthcurver package (version 0.3.1) (Sprouffs and Wagner, 2016; R Core Team, 2019). The impact of $UO_2(NO_3)_2$ on growth was calculated by dividing the empirical area under curve (auc_e) of a growth curve in the presence of uranium by the auc_e of the same replicate in the absence of uranium.

2.3. Interaction of *C. metallidurans* NA4 with uranium

Three independent stationary phase cultures grown in RM medium for two days were pelleted for 5 min at 8500 g (Eppendorf centrifuge 5804R), washed with 10 mM $MgSO_4$ and diluted to a cell concentration

of 10^9 cells/mL ($OD_{600} = 1$) in RM medium. Each suspension was split in two and diluted 10 times in RM medium in culture flasks (Cellstar cell culture flasks 250 mL) with a final volume of 60 mL. Half of the suspensions were supplemented 75 μ M carbonyl cyanide m-chlorophenyl hydrazone (CCCP, Sigma-Aldrich, Belgium) to metabolically inactivate the cultures by blocking the electron transport chain. In addition, three abiotic replicates, without cells, were prepared as a control. $UO_2(NO_3)_2$ was added to a final concentration of 100 μ M to all replicates. Cultures were incubated in the dark at 30 °C on a 180 rpm rotary shaker. Samples were taken at 0, 6 and 24 h for determining viable and total counts, inductively coupled plasma-mass spectrometry (ICP-MS), transmission electron microscopy (TEM HAADF-EDX) and ion chromatography (IC).

2.3.1. Viable counts

Samples were vortexed horizontally for 2 min, diluted ten times in Ringer solution (2.25 g/L NaCl, 0.105 g/L KCl, 0.12 g/L $CaCl_2$, 0.05 g/L $NaHCO_3$ and 0.05% Tween-20) and vortexed again for 2 min. A ten-fold dilution series prepared in Ringer solution was plated on RM agar plates, incubated at 30 °C and colony forming units (CFU) were counted after 3 days.

2.3.2. Total cell count

Total cell counts were performed via flow cytometry. Samples were diluted in 0.2 μ m filter-sterilized (acrodisc syringe filters 25 mm, Pall corporation, USA) bottled mineral Evian water and double-stranded DNA was stained with SYBR Green I (10,000x concentrate in 0.2 μ m filtered dimethyl sulfoxide, ThermoFisher Scientific, Belgium) (final concentration 1x). Samples were incubated for 20 min at 37 °C in dark conditions and each sample was run for 50 μ L with a threshold of 1000 on FL-1 H on a C6 Accuri Flow Cytometer (BD, Erembodegem, Belgium), which was equipped with four fluorescence detectors (530/30 nm, 585/40 nm, >670 nm and 675/25 nm), two scatter detectors and a 20 mW 488 nm laser. PhenoFlow package for R (Props et al., 2016) was used for gating and event counting.

2.3.3. Inductively coupled plasma-mass spectrometry analysis

Ten mL of each culture was centrifuged for 5 min at 8500 g (Rotina 420 R, Hettich). The supernatant was transferred to a new falcon tube, acidified with 65% HNO_3 to a final concentration of 2% and filtered through a 0.45 μ m filter (Acrodisc 25 mm Syringe Filter, Pall Corporation) before analysis with an Xseries 2 ICP-MS (Thermo Fischer Scientific). The spectrometer contains an ESI autosampler with a fast valve, a PFA-ST atomizer and a glass spray chamber for liquid samples. Samples were measured in STD-mode and Th was used as an internal standard to correct for possible drift or matrix-effects.

2.3.4. Transmission electron microscopy

After 24 h growth in the presence of 100 μ M $UO_2(NO_3)_2$, samples were pelleted (5 min 8500 g, Rotina 420 R, Hettich), washed twice with 0.1 M sodium perchlorate (VWR) and fixed at 4 °C for 24 h in 0.1 M sodium cacodylate trihydrate (Sigma-Aldrich) with 2.5% glutaraldehyde (vol/vol, Sigma-Aldrich) pH 7.2. Afterwards, cells were dissolved in 0.2 M sodium cacodylate trihydrate and post-fixed in 2% OsO_4 (vol/vol) at 4 °C. Samples were dehydrated in graded concentrations of ethanol and embedded in Epon resin. Ultra-thin sections (70 nm) were deposited on copper grids and observed on a Scanning Transmission Electron Microscopy of High Resolution HAADF FEI TITAN G2 (Chem-iSTEM, FEI, Oregon, USA). The composition of uranium complexes was analyzed by microanalysis with X-ray energy dispersion (EDX).

2.3.5. Ion chromatography

Samples were filtered through a 0.45 μ m filter (Acrodisc 25 mm Syringe Filter, Pall Corporation) and stored at -20 °C until analysis. Glycerol phosphate, present in RM medium, and phosphate, present because of glycerol phosphate hydrolysis, were measured with a Dionex ICS2500 ion chromatography system packed with an IonPac AS11-HS

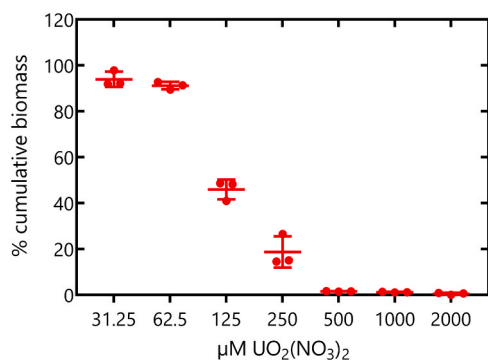


Fig. 1. Growth of *C. metallidurans* strain NA4 in the presence of different uranium concentrations. Data is shown as the percentage of cumulative biomass based on *auc_e* after 72 h with three replicates.

anion exchange column. The eluent gradient program was 1 mM sodium hydroxide for 8 min, increasing to 15 mM sodium hydroxide during the following 10 min, increasing to 30 mM sodium hydroxide in the following 10 min, in the next 10 min increasing to 60 mM sodium hydroxide and finally hold for 2 min at 60 mM sodium hydroxide. Results were analyzed with the Chromeleon V6.50 software.

2.4. Whole genome expression analysis

Three independent stationary phase cultures of *C. metallidurans* NA4 were diluted 1/500 in 50 mL RM medium. The cultures were incubated at 30 °C 120 rpm until a cell concentration of 6×10^8 cells/mL ($OD_{600} = 0.6$) was reached. Then, cultures were divided into two equal subcultures of 25 mL in new falcon tubes. To one of the subcultures, 100 μ M $UO_2(NO_3)_2$ was added, while 100 μ M HCl was added to the other subculture as control. Immediately after addition, the subcultures were incubated for 30 min in the same conditions as before. Next, subcultures were subdivided into 2 mL portions and centrifuged for 5 min at 12,000 g. The supernatant was discarded and pellets were snap frozen in liquid

nitrogen and kept at -80 °C at all times. RNA was extracted from the pellets using the Promega SV total RNA isolation system (Promega, The Netherlands). RNA sequencing (directional mRNA library, RiboZero rRNA depletion and 2×125 bp paired-end sequencing) was performed by Eurofins Genomics GmbH (Ebersberg, Germany). The RNA-seq datasets generated and analyzed for this study are available from the NCBI Sequence Read Archive under accession number PRJNA707064.

Read alignment to the *C. metallidurans* NA4 genome (v2 MaGe platform (Vallet et al., 2013)) and strand-specific read counting (featureCounts) were done with the Rsubread package for R (Liao et al., 2019). Differential gene expression of the resulting count matrix was accomplished using edgeR (Robinson et al., 2009) and limma (Ritchie et al., 2015), using a Benjamini–Hochberg approach to control for Type 1 statistical errors. Genes were found to be differentially expressed if they show a \log_2 fold change higher than 1 or lower than -1 and a p-value lower than 0.05. Further analysis was performed based on the eggNOG functional classification (Powell et al., 2012), downloaded from the MaGe platform (Vallet et al., 2013), and p-values were calculated using the R MLP package (version 1.34.0) on classes with known function (Raghavan et al., 2019).

3. Results & discussion

3.1. *C. metallidurans* NA4 exhibits an active mechanism to precipitate uranium intracellularly as uranium-phosphate associated with PHB

The impact of uranium on the growth of *C. metallidurans* NA4 was investigated by following the optical density in the presence of different concentrations of $UO_2(NO_3)_2$. Growth was not affected up to 62.5 μ M uranium, severely impaired at 125 μ M and 250 μ M, and completely inhibited from 500 μ M onwards (Fig. 1). Next, the interaction and removal was investigated by following growth in the presence and absence of 100 μ M uranium. To differentiate between active and passive mechanisms, CCCP, a chemical known to inhibit the proton motive force and resistance-nodulation-division (RND) efflux pumps (Ikonomidis et al., 2008; Pagès et al., 2005), was added to inactivate the metabolic activity of NA4.

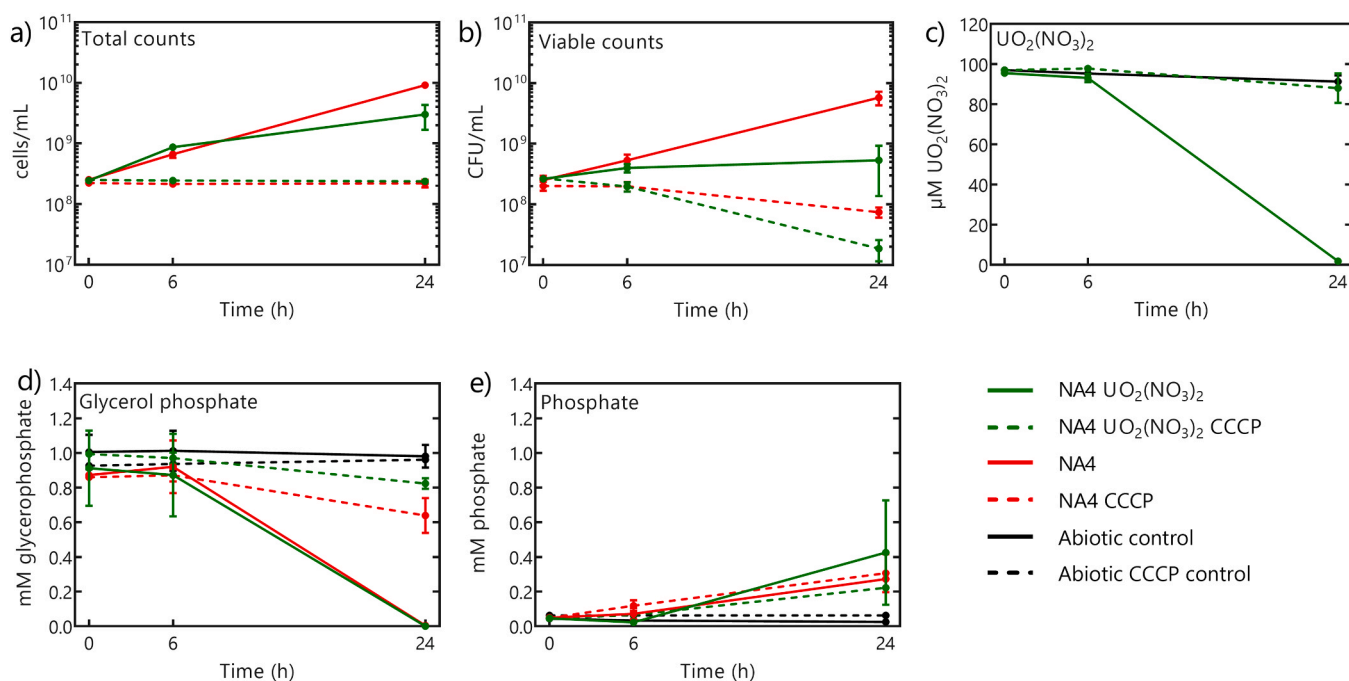


Fig. 2. Growth of *C. metallidurans* NA4 in the presence of uranium. Total (a) and viable (b) counts, concentration of $UO_2(NO_3)_2$ (c), glycerol 2-phosphate (d) and phosphate (e) in the supernatant. Abiotic controls are not visible in a) and b), no abiotic cccp control is presented in c). Values represent the average and standard deviation of three replicates.

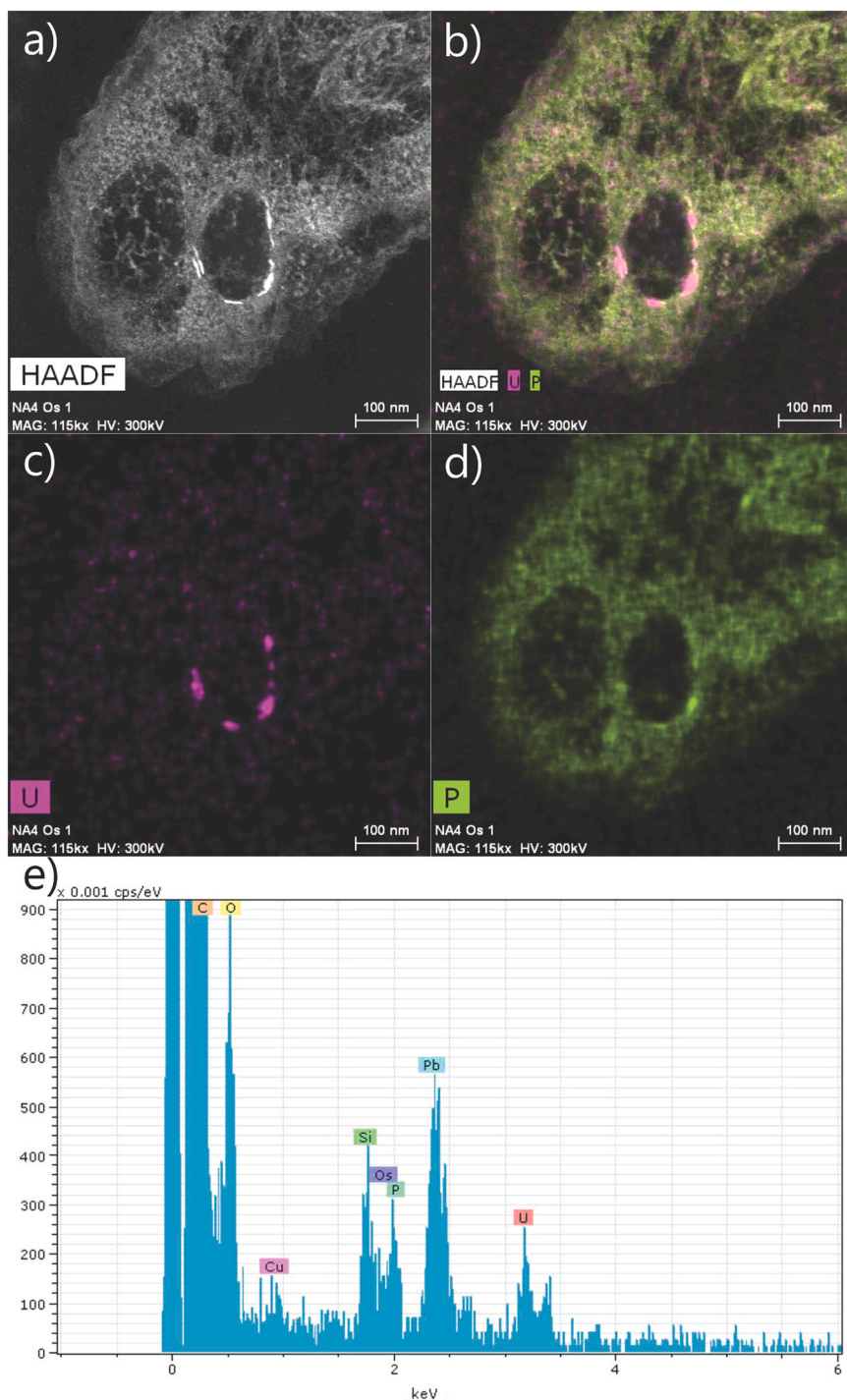


Fig. 3. TEM analysis of the interaction between *C. metallidurans* NA4 and uranium. Transmission electron micrographs of a thin section of *C. metallidurans* NA4 cells after growth for 24 h in the presence of 100 μM $UO_2(NO_3)_2$. (a) HAADF-STEM micrograph together with distribution analysis of (b) uranium (purple) and phosphorus (green), (c) uranium and (d) phosphorus. (e) EDX spectra of a uranium structure near the PHB envelope. The characteristic peaks of copper in the EDX spectra are caused by fluorescence excitation of the TEM support grid. The lead (Pb) peak in the EDX spectrum originated from the lead citrate solution used to improve the visualization of the uranium-treated thin cell sections (Merroun et al., 2005).

Growth was observed in the presence and absence of uranium (Fig. 2a). However, cultures without uranium ($9.2 \times 10^9 \pm 6.5 \times 10^8$ cells/mL) contained approximately three times more cells than the cultures with uranium ($3.0 \times 10^9 \pm 1.3 \times 10^9$ cells/mL) after 24 h. This illustrates the toxic effect of uranium as it impacted final cell density. The difference is even more pronounced when evaluating viable counts (Fig. 2b). Roughly ten times more viable cells were observed without uranium ($5.8 \times 10^9 \pm 1.5 \times 10^9$ CFU/mL) than with uranium ($5.3 \times 10^8 \pm 3.9 \times 10^8$ CFU/mL) at 24 h. In the presence of CCCP, the total number of cells was constant (Fig. 2a), while the number of viable cells decreased on average four times more for cultures with uranium ($1.9 \times 10^7 \pm 7.5 \times 10^6$ CFU/mL versus $7.5 \times 10^7 \pm 1.4 \times 10^7$ CFU/mL)

after 24 h.

Uranium was not removed from the medium after 6 h, while $98 \pm 1\%$ was removed after 24 h (Fig. 2c). No uranium removal was observed in the CCCP-treated NA4 cultures (Fig. 2c), indicating that *C. metallidurans* NA4 actively captures uranium via a metabolic-dependent mechanism. TEM analysis at the 24 h time point indicated that uranium is located intracellular and mainly associated with polyhydroxybutyrate (PHB, Fig. 3a). No extracellular uranium precipitates were observed. Furthermore, EDX analysis revealed a correlation between uranium and phosphorus (Fig. 3b-e), suggesting the complexation of uranium with phosphate. Ion chromatography showed that glycerol 2-phosphate, a component of the growth medium, was completely

hydrolyzed after 24 h with an increase in free phosphate but no difference was seen with or without uranium (Fig. 2d and e). The CCCP-treated cultures also showed a decrease in glycerol phosphate, but to a much lesser extent, which supports the inhibited metabolic activity. Furthermore, the total concentration of glycerol-2 phosphate and free phosphate was constant for the CCCP-treated cultures, indicating no uptake by the cells. Glycerol phosphate, at a ten times higher concentration, has been used previously for extracellular uranium-phosphate precipitation under anaerobic and fermentative conditions (Newsome et al., 2015). However, even though phosphate is released in the medium, no extracellular uranium precipitation was observed in our conditions (Fig. 2c). Possibly, extracellular precipitates were under the detection limit of the TEM-EDX analysis. Furthermore, organic acids are known to influence uranium biomineralization (Tu et al., 2019). Gluconate could thus interfere with extracellular uranium-phosphate precipitation.

The active uranium-phosphate complexation observed in this study differs from the passive biosorption of uranium-phosphate and uranium-carboxylate observed in *C. metallidurans* type strain CH34 at pH 1 and 7 (Llorens et al., 2012). Experiments were performed with Citrate Salt Medium (CSM), which results in a different growth profile compared to routinely used Tris-buffered medium and also RM medium without uranium (Llorens et al., 2012). Uranium-citrate was the major form in the CSM medium and this probably differed from the available uranium complex in RM medium as only a limited amount of citrate is present. This could have impacted the way *C. metallidurans* interacts with uranium.

Uranium-phosphate complexation in bacteria, e.g. mediated by phosphatases, has often been described (Yung and Jiao, 2014; Pinel-Cabello et al., 2021; Kulkarni et al., 2016). However, the association of uranium-phosphate with PHB has not yet been observed. PHB is commonly produced under nutrient starving conditions, such as nitrogen, phosphate or oxygen while encountering an excess of carbon (Schlegel et al., 1961; Third et al., 2003; Oliveira-Filho et al., 2020). It is therefore mainly thought to function as carbon storage, however, a wider protective role has been shown (Müller-Santos et al., 2020). PHB was found to protect moderate levels of oxidative stress, heating and Cu^{2+} stress (Kamnev et al., 2012; Obruca et al., 2016, 2010). Furthermore, simultaneous PHB and polyphosphate (polyP) accumulation has been observed (Doi et al., 1989). PolyP has also been found to be associated with membrane-associated short-chain PHB (Reusch, 2012; Reusch and Sadoff, 1988) and uranium (Merroun et al., 2003, 2006). PHB granules in *C. metallidurans* NA4 might therefore serve as nucleation centers for uranium-phosphate complexation. This intracellular uranium-phosphate bioaccumulation mechanism is promising for bioremediation purposes as uranium-phosphate is less prone to remobilization through reoxidation (Romanchuk et al., 2020; Williamson et al., 2014).

3.2. Uranium induces broad changes in the transcriptome

To gain more insights into the effect of uranium on the transcriptome, RNA-seq was performed after exposure of *C. metallidurans* strain NA4 to 100 μM $\text{UO}_2(\text{NO}_3)_2$ for 30 min and compared to unexposed cells. This resulted in 447 up- and 331 downregulated genes. Differentially expressed genes were mostly located on the chromid, followed by the chromosome and the different plasmids. No significant differentially expressed genes were present on plasmid pNA4_C (Fig. 4).

EggNOG functional classification combined with the MLP R package was used to explore the functional relevance of the differentially expressed genes. Genes of different classes were differentially expressed and nine classes were significantly over-represented (Fig. 5), in order of decreasing significance: inorganic ion transport and metabolism (class P), amino acid transport and metabolism (class E), signal transduction mechanisms (class T), cell wall/membrane/envelope biogenesis (class M), posttranslational modification, protein turnover, chaperones (class

O), energy production and conversion (C), secondary metabolites biosynthesis, transport and catabolism (class Q), cell motility (class N) and defense mechanisms (class V). Upregulated genes of classes P, T, Q and some genes of class M are involved in metal detoxification. Classes V, C, N, E and O corresponded more to general stress responses or possible non-specific inductions.

3.2.1. General stress responses

C. metallidurans NA4 harbors 48 two-component regulatory systems (TCSs) (class T), which play an important role in the ability to respond to changing environmental stimuli by modifying gene expression levels (Laub and Goulian, 2007). Transcription of 10 TCSs was upregulated including one of the EnvZ-OmpR-family TCSs (Table S1). This family of TCSs typically responds to osmolarity changes by regulating the expression of the outer membrane porins (Cai and Inouye, 2002), but non-canonical responses have also been identified (Kenney and Anand, 2020). The induced *envZ-ompR* copy is located adjacent to an upregulated multidrug efflux system (*mdtCBA*, class V). Possibly, EnvZ-OmpR regulates this RND-type efflux system in *C. metallidurans* and was upregulated as a general stress response.

Upregulated genes associated with energy production and conversion (class C) were mainly involved in nitrite and nitrate reduction (*nir* and *nar* genes), presumably because of the upregulation of *narLX*, while cytochrome *c* and cytochrome *c* oxidases were found up- and downregulated (Table S1). Cytochrome *c* is known to have a prominent role in uranium reduction in several species (Holmes et al., 2009; Anderson et al., 2003; Shelobolina et al., 2007, 2008; Payne et al., 2004). However, reduction of uranium or nitrate is not expected in an aerobic environment. Furthermore, if uranium is reduced to U^{+4} , oxygen allows a fast re-oxidation to U^{+6} (Braeken et al., 2006).

Flagellar and chemotaxis genes (class N) were downregulated, which was also observed in *S. bentonitica* BII-R7 in response to uranium (Pinel-Cabello et al., 2021). Heat shock proteins, proteases and peptidases (class O) were also upregulated, probably as a stress response to protect and/or regulate the proteome during uranium exposure. Amino acid ABC-type transporters (class E), such as branched chain amino acid transporters *livFGMHK* and dipeptide transporters *dppFDA*, and secondary metabolites biosynthesis, transport and catabolism (class Q), such as phenol hydroxylase *dmpLMNO* and phenylacetyl-CoA ligase *paaK* (Table S1) were also downregulated.

In *Caulobacter crescentus*, a mutant lacking ppGpp synthetase/hydrolase *spoT* was found to have a lower survival rate under U stress in carbon starvation conditions (Yung et al., 2015). PpGpp has been designated as a global regulator to aid adaptation of an organism to environmental conditions, as reviewed in (Cavalheiro et al., 2009). In *C. metallidurans* NA4, *spoT* was not differentially expressed, presumably since RNA-seq was not performed under carbon starvation conditions. However, this does not refute a role for *spoT* in carbon starvation conditions.

3.2.2. PHB and phosphate metabolism

A TCS of the OmpR/winged helix family (CmetNA4_v1_pm2511–2512) was upregulated and found in the vicinity of upregulated genes coding for an aldehyde dehydrogenase (*aldB*), an acetoacetyl-CoA reductase (*phaB*), a poly-beta-hydroxybutyrate polymerase (*phaC*) and unknown functions (Table S1). A second copy of the *pha* locus was not differentially expressed (CmetNA4_v2_2218–2220). PHB production has been investigated extensively in *Cupriavidus necator* (Yang et al., 2009). PHB granules are covered with proteins such as PhaC, involved in PHB biosynthesis, PhaZ, which can hydrolyze PHB or induce PHB thiolysis under carbon starvation, and phasins (PhaPs), amphiphilic polypeptides with an undefined role (Müller-Santos et al., 2020). The regulation of these phasins is attributed to the negative transcriptional regulator PhaR, which also binds to the PHB surface to decrease the amount of DNA-bound PhaR. In *C. metallidurans* NA4, PhaR (CmetNA4_v2_2222) was not differentially expressed after exposure to

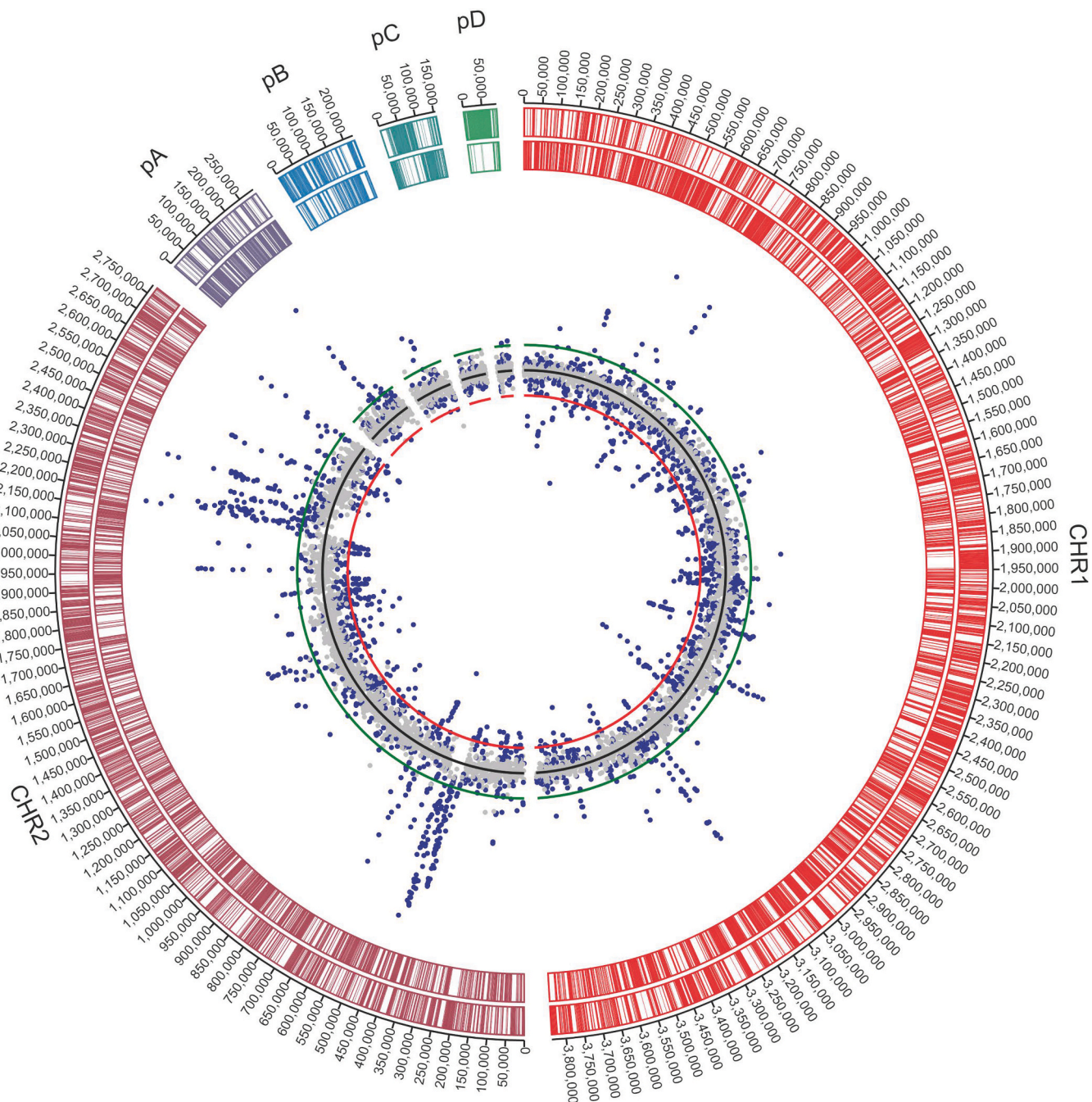


Fig. 4. Scatter plot of RNA-Seq-derived gene expression in *C. metallidurans* NA4 after 100 μM uranium exposure compared to non-induced conditions. Dots represent \log_2 ratios (blue $p < 0.05$) with red, black, and green lines corresponding to -1 , 0 , and 1 , respectively. (CHR1: chromosome; CHR2: chromid; pA: plasmid pNA4_A; pB: plasmid pNA4_B; pC: plasmid pNA4_C; pD: plasmid pNA4_D).

uranium, but the unidentified TCS (CmetNA4_v1_pm2511–2512) might regulate carbon metabolism related to PHB production by inducing *phab* and *phaC* expression (Table S1).

The involvement of phosphatases is often observed and suggested to play an essential role in uranium-phosphate complexation (Hu et al., 2005; Yung and Jiao, 2014; Pinel-Cabello et al., 2021; Theodorakopoulos et al., 2015). However, phosphatases were not differentially expressed after uranium induction in *C. metallidurans* NA4. Moreover, a glycerol 3-phosphate transporter (*ugpBAEC*, CmetNA4_v2_3084–3087) and a cytosolic glycerophosphodiester phosphodiesterase (*ugpQ*, CmetNA4_v2_3083) were found to be downregulated. While *ugpBAECQ* is designated as a glycerol 3-phosphate transporter, it has also been suggested that it can recognize glycerol 2-phosphate as a substrate in *E. coli*

K-12 (Orellana et al., 2014). This could mean that glycerol 2-phosphate uptake is reduced so that extracellular hydrolysis is preferred. Glycerol 2-phosphate is presumably hydrolyzed by phosphatases such as the secreted CmetNA4_v2_3680, periplasmic CmetNA4_v1_pm0542, *phoA* (CmetNA4_v1_pm1046–1047), and CmetNA4_v1_pA0287–0288 or cytoplasmic membrane associated CmetNA4_v2_0397. However, it is not presumed to have a big impact in these conditions since glycerol 2-phosphate was present in excess and no difference in hydrolysis rate was observed in our experiments with/without uranium (Fig. 2d). Furthermore, considering the downregulation of *ugpBAECQ* and the release of free phosphate during our experiments (Fig. 2e), the secreted phosphatase CmetNA4_v2_3680 is suggested to have a major contribution to the hydrolysis of glycerol 2-phosphate.

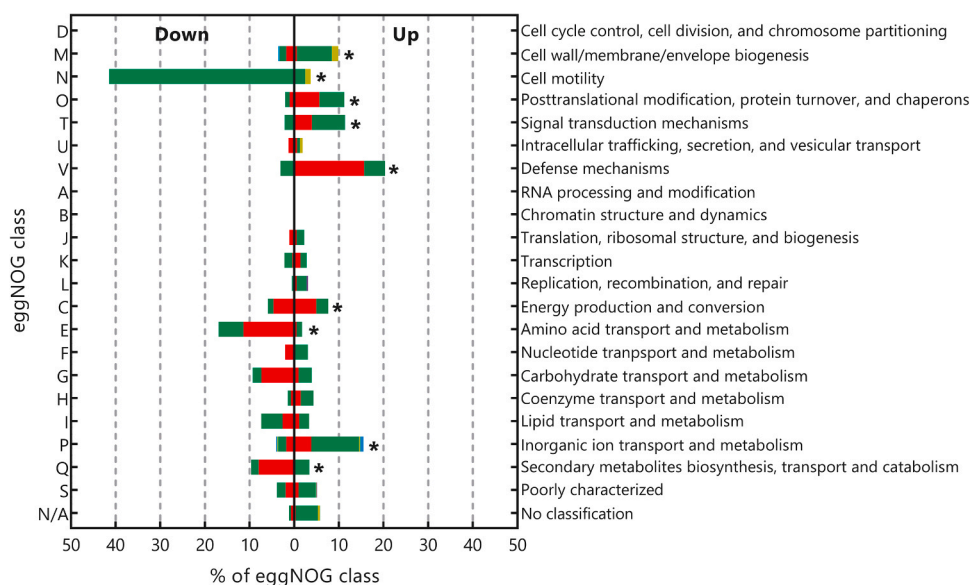


Fig. 5. EggNOG classification of differentially expressed genes. Gene expression of NA4 induced with 100 μ M uranium compared to non-induced conditions. Percentages were calculated by dividing the number of genes in a certain category by the total number of genes in that category and then colored by replicon. Genes on replicon CHR1 are shown in red, CHR2 in green, pA in light green, pB in blue and pD in purple. No significant differentially expressed genes were present on pC. Asterisks indicate significant ($p < 0.05$) classes based on the MLP package.

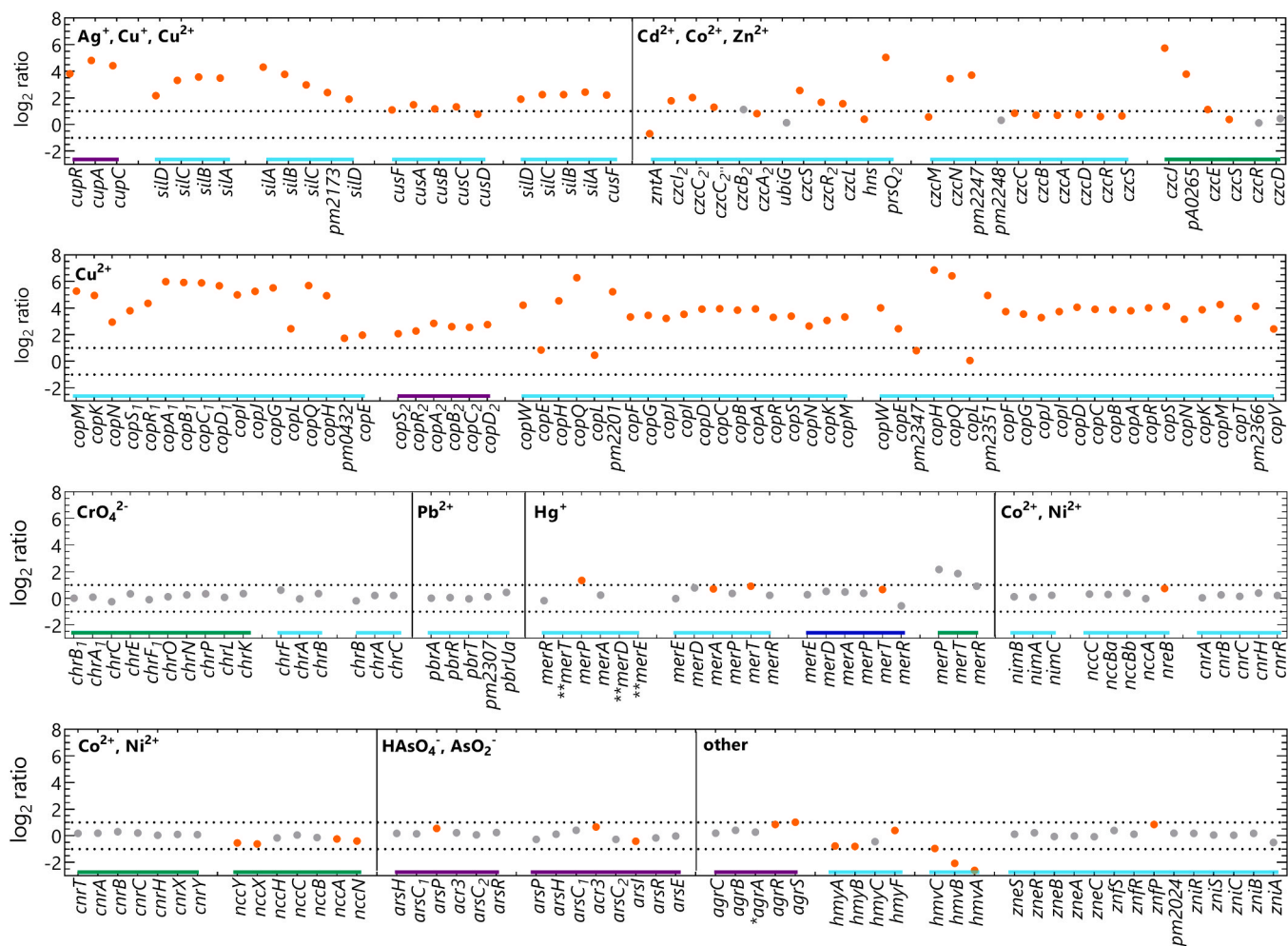


Fig. 6. Metal detoxification genes. Overview of all metal detoxification genes present in *C. metallidurans* NA4. Significant (orange dots; $p < 0.05$) and non-significant (grey dots) \log_2 ratios are shown for known metal resistance genes located on the chromosome (purple line under the graph), chromid (light blue), pA (dark blue), and pB (green). Dotted lines correspond to -1 and 1 , respectively. *non-functional genes. **NA.

3.2.3. Metal detoxification genes

Cupriavidus metallidurans NA4 harbors a wide plethora of metal resistance genes of which several are induced after uranium induction (Fig. 6). Although specific uranium efflux mechanisms have not yet been described, genes encoding RND-type systems were upregulated in *Stenotrophomonas bentonitica* and *Geobacter sulfurreducens* after uranium induction (Pinel-Cabello et al., 2021; Nies et al., 1987). For *G. sulfurreducens*, *czcABC*, involved in cadmium, zinc and cobalt resistance (Mergeay et al., 1985; Nongkhlaw and Joshi, 2019), was upregulated, while in *S. bentonitica* only *czcA* was upregulated during the exponential phase. In *Chryseobacterium* sp. *PMSZPI*, *czcA* was also upregulated in the presence of 0.5 mM uranium (Monsieurs et al., 2011). *C. metallidurans* NA4 harbors two *czc* gene clusters, both located on the chromid. One cluster (CmetNA4_v1_pm2249–2254) was not differentially expressed. The second cluster (CmetNA4_v1_pm0610–0620) was upregulated, probably mediated via the upregulated cognate TCS CzcR₂S₂ (Table S1). However, *czcC*₂ carries a 2-bp deletion, which results in an abnormal short protein (207 instead of 432 residues) and putatively inactive CzcC₂B₂A₂ pump. Therefore, although CzcCBA seems responsive towards uranium, its role in *C. metallidurans* NA4 is currently uncertain. Further research is necessary to investigate a possible role in uranium resistance. Noticeably, almost all genes (from 9 different clusters) involved in the response to and detoxification of silver and copper were upregulated (Fig. 6). However, a link between uranium and copper or silver resistance is not yet known. Putatively, uranium induced the expression of several TCSs (*czcR*₂S₂, *copR*₂S₂ and three copies of *copRS*), which on its turn resulted in the upregulation of their target regulations. Moreover, possible cross-regulation between metal-responsive TCSs has been shown [79].

Other metal resistance gene clusters were not clearly up- or down-regulated. However, uranium has been shown to impact iron metabolism with a possible role for siderophores (Gallois et al., 2018; Nies et al., 1987). The iron-related response in *C. metallidurans* NA4 was ambiguous. Most iron metabolism genes, such as siderophores, were not differentially expressed, only a 4Fe-4S ferredoxin (CmetNA4_v2_3073), ferric uptake regulation protein (*fur*, CmetNA4_v1_pm2192) and ferric aerobactin receptor (*iutA*, CmetNA4_v1_pm2186) were upregulated while three other ferredoxins (CmetNA4_v2_1971, CmetNA4_v1_pm1751–1752) and a putative periplasmic binding component involved in Fe³⁺ transport (CmetNA4_v1_pm0053) were downregulated (Table S1).

4. Conclusions

Although uranium hampered cell growth, *C. metallidurans* NA4 was able to remove uranium from the medium as uranium-phosphate complexes via an active mechanism. It was shown for the first time that these complexes were mainly associated with PHB, which might serve as a nucleation center for uranium-phosphate precipitation. The toxic effect of uranium was further confirmed by whole transcriptome sequencing after uranium induction, which revealed a broad response. Overall, genes encoding general stress-related proteins were upregulated such as a multidrug efflux system and heat shock proteins. Phosphatases are often linked with forming uranium-phosphate precipitates; however we could not identify a clear link with phosphate metabolism and the observed uranium-phosphate precipitates. The association of PHB granules with uranium phosphate precipitates could have been facilitated by the upregulation of a poly-beta-hydroxybutyrate polymerase (*phaC*). Gene clusters involved in copper and silver resistance were upregulated together with some genes related to cadmium, cobalt and zinc resistance, while gene clusters involved in chromium, lead, mercury, nickel and arsenic resistance were not differentially expressed. The complex transcriptional response could be facilitated by the upregulation of 10 TCSs, of which five are known to be involved in metal resistance and are able to cross-regulate different genes. Such a versatile transcriptional network probably enables *C. metallidurans* species to

thrive in environments contaminated with multiple metals. Altogether, our results bring further insights on interaction mechanisms of microorganisms with uranium, together with a better understanding of the molecular uranium response. The active uranium bioaccumulation process of the multi-metal resistant bacterium *C. metallidurans* NA4 is promising for uranium bioremediation purposes. Nevertheless, bioremediation applications could benefit from additional studies in a multiple metal environment to further unravel possible co-resistance/sensitivity between different metals.

CRedit authorship contribution statement

Tom Rogiers: Conceptualization, Data curation, Formal analysis, Methodology, Writing – original draft. **Mohamed L. Merroun:** TEM analysis, Investigation, Writing – review & editing. **Adam Williamson:** Methodology, Writing – review & editing. **Natalie Leys:** Resources. **Rob Van Houdt:** Conceptualization, Methodology, Writing – review & editing. **Nico Boon:** Methodology, Writing – review & editing. **Kristel Mijndonckx:** Conceptualization, Methodology, Writing – review & editing, Project administration.

Declaration of Competing Interest

The authors declare that they have no known competing financial interests or personal relationships that could have appeared to influence the work reported in this paper.

Acknowledgments

This project was funded by SCK CEN (Belgium) through the PhD project of Tom Rogiers.

Appendix A. Supporting information

Supplementary data associated with this article can be found in the online version at doi:10.1016/j.jhazmat.2021.126737.

References

- IAEA, Extent of Environmental contamination by naturally occurring radioactive material (NORM) and technological options for mitigation, 2003.
- Ma, M., Wang, R., Xu, L., Xu, M., Liu, S., 2020. Emerging health risks and underlying toxicological mechanisms of uranium contamination: lessons from the past two decades. *Environ. Int.* 145, 106107 <https://doi.org/10.1016/j.envint.2020.106107>.
- Rogiers, T., Claesen, J., Van Gompel, A., Vanhoudt, N., Mysara, M., Williamson, A., Leys, N., Van Houdt, R., Boon, N., Mijndonckx, K., 2021. Soil microbial community structure and functionality changes in response to long-term metal and radionuclide pollution. *Environ. Microbiol.* 23, 1670–1683. <https://doi.org/10.1111/1462-2920.15394>.
- Francis, A.J., Gillow, J.B., Dodge, C.J., Harris, R., Beveridge, T.J., Papenguth, H.W., 2004. Uranium association with halophilic and non-halophilic bacteria and archaea. *Radiochim. Acta* 92, 481–488. <https://doi.org/10.1524/ract.92.8.481.39281>.
- Suzuki, Y., Kelly, S.D., Kemner, K.M., Banfield, J.F., 2005. Direct microbial reduction and subsequent preservation of uranium in natural near-surface sediment. *Appl. Environ. Microbiol.* 71, 1790–1797. <https://doi.org/10.1128/AEM.71.4.1790>.
- Beller, H.R., 2005. Anaerobic, nitrate-dependent oxidation of U (IV) oxide minerals by the chemolithoautotrophic bacterium *Thiobacillus denitrificans*. *Appl. Environ. Microbiol.* 71, 2170–2174. <https://doi.org/10.1128/AEM.71.4.2170>.
- Suzuki, Y., Banfield, J.F., 2004. Resistance to, and accumulation of, uranium by bacteria from a uranium-contaminated site. *Geomicrobiol. J.* 21, 113–121. <https://doi.org/10.1080/01490450490266361>.
- Jroundi, F., Merroun, M.L., Arias, J.M., Rossberg, A., Selenska-Pobell, S., González-Muñoz, M.T., 2007. Spectroscopic and microscopic characterization of uranium biomineralization in *Myxococcus xanthus*. *Geomicrobiol. J.* 24, 441–449. <https://doi.org/10.1080/01490450701437651>.
- Martinez, R.J., Beazley, M.J., Taillefert, M., Arakaki, A.K., Skolnick, J., Sobczyk, P.A., 2007. Aerobic uranium (VI) bioprecipitation by metal-resistant bacteria isolated from radionuclide- and metal-contaminated subsurface soils. *Environ. Microbiol.* 9, 3122–3133. <https://doi.org/10.1111/j.1462-2920.2007.01422.x>.
- Carvajal, D.A., Katsenovich, Y.P., Lagos, L.E., 2012. The effects of aqueous bicarbonate and calcium ions on uranium biosorption by *Arthrobacter* G975 strain. *Chem. Geol.* 330–331, 51–59. <https://doi.org/10.1016/j.chemgeo.2012.08.018>.

- Merroun, M.L., Selenska-Pobell, S., 2008. Bacterial interactions with uranium: an environmental perspective. *J. Contam. Hydrol.* 102, 285–295. <https://doi.org/10.1016/j.jconhyd.2008.09.019>.
- Lopez-Fernandez, M., Vilchez-Vargas, R., Jroundi, F., Boon, N., Pieper, D., Merroun, M. L., 2018. Microbial community changes induced by uranyl nitrate in bentonite clay microcosms. *Appl. Clay Sci.* 160, 206–216. <https://doi.org/10.1016/j.clay.2017.12.034>.
- Sutcliffe, B., Chariton, A.A., Harford, A.J., Hose, G.C., Greenfield, P., Elbourne, L.D.H., Oytam, Y., Stephenson, S., Midgley, D.J., Paulsen, I.T., 2017. Effects of uranium concentration on microbial community structure and functional potential. *Environ. Microbiol.* 19, 3323–3341. <https://doi.org/10.1111/1462-2920.13839>.
- Hillson, N.J., Hu, P., Andersen, G.L., Shapiro, L., 2007. *Caulobacter crescentus* as a whole-cell uranium biosensor. *Appl. Environ. Microbiol.* 73, 7615–7621. <https://doi.org/10.1128/AEM.01566-07>.
- Macaskie, L.E., Bonthron, K.M., Yong, P., Goddard, D.T., 2000. Enzymically mediated bioprecipitation of uranium by a *Citrobacter* sp.: a concerted role for exocellular lipopolysaccharide and associated phosphatase in biomineral formation. *Microbiology* 146, 1855–1867. <https://doi.org/10.1099/00221287-146-8-1855>.
- Beazley, M.J., Martinez, R.J., Sobocky, P.A., Webb, S.M., Taillefer, M., 2007. Uranium biomineralization as a result of bacterial phosphatase activity: Insights from bacterial isolates from a contaminated subsurface. *Environ. Sci. Technol.* 41, 5701–5707. <https://doi.org/10.1021/es070567g>.
- Merroun, M.L., Nedelkova, M., Ojeda, J.J., Reitz, T., Fernández, M.L., Arias, J.M., Romero-González, M., Selenska-pobell, S., 2011. Bio-precipitation of uranium by two bacterial isolates recovered from extreme environments as estimated by potentiometric titration, TEM and X-ray absorption spectroscopic analyses. *J. Hazard. Mater.* 197, 1–10. <https://doi.org/10.1016/j.jhazmat.2011.09.049>.
- Hu, P., Brodie, E.L., Suzuki, Y., Mcadams, H.H., Andersen, G.L., 2005. Whole-genome transcriptional analysis of heavy metal stresses in *Caulobacter crescentus*. *J. Bacteriol.* 187, 8437–8449. <https://doi.org/10.1128/JB.187.24.8437>.
- Yung, M.C., Jiao, Y., 2014. Biomineralization of uranium by PhoY phosphatase activity aids cell survival in *Caulobacter crescentus*. *Appl. Environ. Microbiol.* 80, 4795–4804. <https://doi.org/10.1128/AEM.01050-14>.
- Pinel-Cabello, M., Jroundi, F., López-Fernández, M., Geffers, R., Jarek, M., Jauregui, R., Link, A., Vilchez-Vargas, R., Merroun, M.L., 2021. Multisystem combined uranium resistance mechanisms and bioremediation potential of *Stenotrophomonas bentonitica* BH-R7: transcriptomics and microscopic study. *J. Hazard. Mater.* 403, 123858. <https://doi.org/10.1016/j.jhazmat.2020.123858>.
- Yung, M.C., Park, D.M., Wesley Overton, K., Blow, M.J., Hoover, C.A., Smit, J., Murray, S.R., Ricci, D.P., Christen, B., Bowman, G.R., Jiao, Y., 2015. Transposon mutagenesis paired with deep sequencing of *Caulobacter crescentus* under uranium stress reveals genes essential for detoxification and stress tolerance. *J. Bacteriol.* 197, 3160–3172. <https://doi.org/10.1128/JB.00382-15>.
- Gallois, N., Alpha-bazin, B., Ortet, P., Barakat, M., Piette, L., Long, J., Berthomieu, C., Armengaud, J., Chapon, V., 2018. Proteogenomic insights into uranium tolerance of a *Microbacterium* bacterial isolate. *J. Proteom.* 177, 148–157. <https://doi.org/10.1016/j.jprot.2017.11.021>.
- Theodorakopoulos, N., Chapon, V., Coppin, F., Floriani, M., Vercouter, T., Sergeant, C., Camilleri, V., Berthomieu, C., Févriér, L., 2015. Use of combined microscopic and spectroscopic techniques to reveal interactions between uranium and *Microbacterium* sp. A9, a strain isolated from the Chernobyl exclusion zone. *J. Hazard. Mater.* 285, 285–293. <https://doi.org/10.1016/j.jhazmat.2014.12.018>.
- Holmes, D.E., O'Neil, R.A., Chavan, M.A., N'Guessan, L.A., Vronis, H.A., Perpetua, L.A., Larrahondo, M.J., Didonato, R., Liu, A., Lovley, D.R., 2009. Transcriptome of *Geobacter uraniireducens* growing in uranium- contaminated subsurface sediments. *ISME J.* 3, 216–230. <https://doi.org/10.1038/ismej.2008.89>.
- Anderson, R.T., Vronis, H.A., Ortiz-bernad, I., Resch, C.T., Long, P.E., Dayvault, R., Karp, K., Marutzky, S., Metzler, D.R., Peacock, A., White, D.C., Lowe, M., Lovley, D. R., 2003. Stimulating the in situ activity of *Geobacter* Species to remove uranium from the groundwater of a uranium-contaminated aquifer. *Appl. Environ. Microbiol.* 69, 5884–5891. <https://doi.org/10.1128/AEM.69.10.5884>.
- Shelobolina, E.S., Coppi, M.V., Korenevsky, A.A., Didonato, L.N., Sullivan, S.A., Konishi, H., Xu, H., Leang, C., Butler, J.E., Kim, B., Lovley, D.R., 2007. Importance of c-Type cytochromes for U(VI) reduction by *Geobacter sulfurreducens*. *BMC Microbiol* 7, 16. <https://doi.org/10.1186/1471-2180-7-16>.
- Shelobolina, E.S., Vronis, H.A., Findlay, R.H., Lovley, D.R., 2008. *Geobacter uraniireducens* sp. nov., isolated from subsurface sediment undergoing uranium bioremediation. *Int. J. Syst. Evol. Microbiol.* 58, 1075–1078. <https://doi.org/10.1099/ijs.0.65377-0>.
- Shi, L., Belchik, S.M., Wang, Z., Kennedy, D.W., Dohnalkova, A.C., Marshall, M.J., Zachara, J.M., Fredrickson, J.K., 2011. Identification and characterization of UndA HRCR-6, an outer membrane endocytosis c-type cytochrome of *Shewanella* sp. strain HRCR-6. *Appl. Environ. Microbiol.* 77, 5521–5523. <https://doi.org/10.1128/AEM.00614-11>.
- Ghasemi, R., Fatemi, F., Mir-Derikvand, M., Zarei, M., 2020. Evaluation of mtr cluster expression in *Shewanella* RCRI7 during uranium removal. *Arch. Microbiol.* 202, 2711–2726. <https://doi.org/10.1007/s00203-020-01981-1>.
- Ganesh, R., Robinson, K.G., Reed, G.D., Saylor, G., 1997. Reduction of hexavalent uranium from organic complexes by sulfate- and iron-reducing bacteria. *Appl. Environ. Microbiol.* 63, 4385–4391.
- Wang, L., Xiao, S., Chen, X., Chen, S., Wang, S., Wang, C., Tang, Y., Dong, F., 2019. ytiB and ythA genes reduce the uranium removal capacity of *Bacillus atrophaeus*. *Int. J. Mol. Sci.* 20, 1–12. <https://doi.org/10.3390/ijms20071766>.
- Diels, L., Mergeay, M., 1990. DNA probe-mediated detection of resistant bacteria from soils highly polluted by heavy metals. *Appl. Environ. Microbiol.* 56, 1485–1491. <https://doi.org/10.1128/aem.56.5.1485-1491.1990>.
- Mijnendonckx, K., Provoost, A., Ott, C.M., Venkateswaran, K., Mahillon, J., Leys, N., van Houdt, R., 2013. Characterization of the survival ability of *Cupriavidus metallidurans* and *Ralstonia pickettii* from space-related environments. *Microb. Ecol.* 65, 347–360. <https://doi.org/10.1007/s00248-012-0139-2>.
- Ali, M.M., Provoost, A., Maertens, L., Leys, N., Monsieurs, P., Charlier, D., Van Houdt, R., 2019. Genomic and transcriptomic changes that mediate increased platinum resistance in *Cupriavidus metallidurans*. *Genes* 10, 63. <https://doi.org/10.3390/genes10010063>.
- Mijnendonckx, K., Ali, M.M., Provoost, A., Janssen, P., Mergeay, M., Leys, N., Charlier, D., Monsieurs, P., Van Houdt, R., 2019. Spontaneous mutation in the AgrRS two-component regulatory system of *Cupriavidus metallidurans* results in enhanced silver resistance. *Metallomics* 11, 1912–1924. <https://doi.org/10.1039/c9mt00123a>.
- Mergeay, M., Nies, D.H., Schlegel, H.G., Gerits, J., Charles, P., Van Gijsegem, F., 1985. *Alcaligenes eutrophus* CH34 is a facultative chemolithotroph with plasmid-bound resistance to heavy metals. *J. Bacteriol.* 162, 328–334. <https://doi.org/10.1128/jb.162.1.328-334.1985>.
- Biehl, H., Pfening, N., 1981. Isolation of members of the family rhodospirillaceae. In: *The Prokaryotes*. Springer, Berlin, Heidelberg, pp. 267–273. https://doi.org/10.1007/978-3-662-13187-9_14.
- Sprouffs, K., Wagner, A., 2016. Growthcurver: an R package for obtaining interpretable metrics from microbial growth curves. *BMC Bioinforma.* 17, 17–20. <https://doi.org/10.1186/s12859-016-1016-7>.
- R Core Team, R: a language and environment for statistical computing., R Found. Stat. Comput. Vienna, Austria, 2019. (<https://www.r-project.org/>).
- Props, R., Monsieurs, P., Mysara, M., Clement, L., Boon, N., 2016. Measuring the biodiversity of microbial communities by flow cytometry. *Methods Ecol. Evol.* 7, 1376–1385. <https://doi.org/10.1111/2041-210X.12607>.
- Merroun, M.L., Raff, J., Rossberg, A., Hennig, C., Reich, T., Selenska-Pobell, S., 2005. Complexation of uranium by cells and S-layer sheets of *Bacillus sphaericus* JG-A12. *Appl. Environ. Microbiol.* 71, 5532–5543. <https://doi.org/10.1128/AEM.71.9.5532-5543.2005>.
- Vallenet, D., Belda, E., Calteau, A., Cruveiller, S., Engelen, S., Lajus, A., Le Fèvre, F., Longin, C., Mornico, D., Roche, D., Rouy, Z., Salvignol, G., Scarpelli, C., Smith, A.A. T., Weiman, M., Médigue, C., 2013. MicroScope - An integrated microbial resource for the curation and comparative analysis of genomic and metabolic data. *Nucleic Acids Res.* 41, 636–647. <https://doi.org/10.1093/nar/gks1194>.
- Liao, Y., Smyth, G.K., Shi, W., 2019. The R package Rsubread is easier, faster, cheaper and better for alignment and quantification of RNA sequencing reads. *Nucleic Acids Res.* 47, e47. <https://doi.org/10.1093/nar/gkz114>.
- Robinson, M.D., McCarthy, D.J., Smyth, G.K., 2009. edgeR: A Bioconductor package for differential expression analysis of digital gene expression data. *Bioinformatics* 26, 139–140. <https://doi.org/10.1093/bioinformatics/btp616>.
- Ritchie, M.E., Phipson, B., Wu, D., Hu, Y., Law, C.W., Shi, W., Smyth, G.K., 2015. Limma powers differential expression analyses for RNA-sequencing and microarray studies. *Nucleic Acids Res.* 43, 47. <https://doi.org/10.1093/nar/gkv007>.
- Powell, S., Szklarczyk, D., Trachana, K., Roth, A., Kuhn, M., Müller, J., Arnold, R., Rattei, T., Letunic, I., Doerks, T., Jensen, L.J., Von Mering, C., Bork, P., 2012. eggNOG v3.0: Orthologous groups covering 1133 organisms at 41 different taxonomic ranges. *Nucleic Acids Res.* 40, 284–289. <https://doi.org/10.1093/nar/gkr1060>.
- N. Raghavan, T. Verbeke, A. De Bondt, J. Cabrera, D. Amaratunga, T. Casneuf, W. Ligenber, MLP: MLP. R package version 1.34.0, 2019. (<https://www.bioconductor.org/packages/release/bioc/html/MLP.html>).
- Ikonomidis, A., Tsakris, A., Kanellou, M., Maniatis, A.N., Pournaras, S., 2008. Effect of the proton motive force inhibitor carbonyl cyanide-m-chlorophenylhydrazone (CCCP) on *Pseudomonas aeruginosa* biofilm development. *Lett. Appl. Microbiol.* 47, 298–302. <https://doi.org/10.1111/j.1472-765X.2008.02430.x>.
- Pagès, J.M., Masi, M., Barbe, J., 2005. Inhibitors of efflux pumps in Gram-negative bacteria. *Trends Mol. Med.* 11, 382–389. <https://doi.org/10.1016/j.molmed.2005.06.006>.
- Newsome, L., Morris, K., Lloyd, J.R., 2015. Uranium biominerals precipitated by an environmental isolate of *Serratia* under anaerobic conditions. *PLoS One* 10, 1–14. <https://doi.org/10.1371/journal.pone.0132392>.
- Tu, H., Yuan, G., Zhao, C., Liu, J., Li, F., Yang, J., Liao, J., Yang, Y., Liu, N., 2019. U-phosphate biomineralization induced by *Bacillus* sp. dw-2 in the presence of organic acids. *Nucl. Eng. Technol.* 51, 1322–1332. <https://doi.org/10.1016/j.net.2019.03.002>.
- Llorens, I., Untereiner, G., Jaillard, D., Gouget, B., Chapon, V., Carriere, M., 2012. Uranium interaction with two multi-resistant environmental bacteria: *Cupriavidus metallidurans* CH34 and *Rhodospseudomonas palustris*. *PLoS One* 7, 1–10. <https://doi.org/10.1371/journal.pone.0051783>.
- Kulkarni, S., Misra, C.S., Gupta, A., Ballal, A., Apte, S.K., 2016. Interaction of uranium with bacterial cell surfaces: inferences from phosphatase-mediated uranium precipitation. *Appl. Environ. Microbiol.* 82, 4965–4974. <https://doi.org/10.1128/AEM.00728-16>.
- Schlegel, H.G., Gottschalk, G., Von Bartha, R., 1961. Formation and utilization of poly-β-hydroxybutyric acid by knallgas bacteria (*Hydrogenomonas*). *Nature* 191, 463–465.
- Third, K.A., Newland, M., Cord-Ruwisch, R., 2003. The effect of dissolved oxygen on PHB accumulation in activated sludge cultures. *Biotechnol. Bioeng.* 82, 238–250. <https://doi.org/10.1002/bit.10564>.
- Oliveira-Filho, E.R., Silva, J.G.P., de Macedo, M.A., Taciro, M.K., Gomez, J.G.C., Silva, L. F., 2020. Investigating nutrient limitation role on improvement of growth and poly (3-hydroxybutyrate) accumulation by *Burkholderia sacchari* LMG 19450 from xylose as the sole carbon source. *Front. Bioeng. Biotechnol.* 7, 1–11. <https://doi.org/10.3389/fbioe.2019.00416>.

- Müller-Santos, M., Koskimäki, J.J., Alves, L.P.S., de Souza, E.M., Jendrosseck, D., Pirttilä, A.M., 2020. The protective role of PHB and its degradation products against stress situations in bacteria. *FEMS Microbiol. Rev.* 1–13. <https://doi.org/10.1093/femsre/fuaa058>.
- Kamnev, A.A., Tugarova, A.V., Tarantilis, P.A., Gardiner, P.H.E., Polissiou, M.G., 2012. Comparing poly-3-hydroxybutyrate accumulation in *Azospirillum brasilense* strains Sp7 and Sp245: The effects of copper(II). *Appl. Soil Ecol.* 61, 213–216. <https://doi.org/10.1016/j.apsoil.2011.10.020>.
- Obruca, S., Sedlacek, P., Mravec, F., Samek, O., Marova, I., 2016. Evaluation of 3-hydroxybutyrate as an enzyme-protective agent against heating and oxidative damage and its potential role in stress response of poly(3-hydroxybutyrate) accumulating cells. *Appl. Microbiol. Biotechnol.* 100, 1365–1376. <https://doi.org/10.1007/s00253-015-7162-4>.
- Obruca, S., Marova, I., Svoboda, Z., Mikulikova, R., 2010. Use of controlled exogenous stress for improvement of poly(3-hydroxybutyrate) production in *Cupriavidus necator*. *Folia Microbiol. (Praha)* 55, 17–22. <https://doi.org/10.1007/s12223-010-0003-z>.
- Doi, Y., Kawaguchi, Y., Nakamura, Y., Kunioka, M., 1989. Nuclear magnetic resonance studies of poly(3-hydroxybutyrate) and polyphosphate metabolism in *Alcaligenes eutrophus*. *Appl. Environ. Microbiol.* 55, 2932–2938. <https://doi.org/10.1128/aem.55.11.2932-2938.1989>.
- Reusch, R.N., 2012. Physiological importance of poly-(R)-3-hydroxybutyrates. *Chem. Biodivers.* 9, 2343–2366. <https://doi.org/10.1002/cbdv.201200278>.
- Reusch, R.N., Sadoff, H.L., 1988. Putative structure and function of a poly-β-hydroxybutyrate/calcium polyphosphate channel in bacterial plasma membranes. *Proc. Natl. Acad. Sci. U. S. A.* 85, 4176–4180. <https://doi.org/10.1073/pnas.85.12.4176>.
- Merroun, M., Hennig, C., Rossberg, A., Reich, T., Selenska-Pobell, S., 2003. Characterization of U(VI) – *Acidithiobacillus ferrooxidans* complexes using EXAFS, transmission electron microscopy, and energy-dispersive X-ray analysis. *Radiochim. Acta* 91, 583–591.
- Merroun, M., Nedelkova, M., Rossberg, A., Hennig, C., Selenska-Pobell, S., 2006. Interaction mechanisms of bacterial strains isolated from extreme habitats with uranium. *Radiochim. Acta* 94, 723–729. <https://doi.org/10.1524/ract.2006.94.9-11.723>.
- Romanchuk, A.Y., Vlasova, I.E., Kalmykov, S.N., 2020. Speciation of uranium and plutonium from nuclear legacy sites to the environment: a mini review. *Front. Chem.* 8, 1–10. <https://doi.org/10.3389/fchem.2020.00630>.
- Williamson, A.J., Morris, K., Law, G.T.W., Rizoulis, A., Charnock, J.M., Lloyd, J.R., 2014. Microbial reduction of U(VI) under alkaline conditions: implications for radioactive waste geodisposal. *Environ. Sci. Technol.* 48, 13549–13556. <https://doi.org/10.1021/es5017125>.
- Laub, M.T., Goulian, M., 2007. Specificity in two-component signal transduction pathways. *Annu. Rev. Genet.* 41, 121–145. <https://doi.org/10.1146/annurev.genet.41.042007.170548>.
- Cai, S.J., Inouye, M., 2002. EnvZ-OmpR interaction and osmoregulation in *Escherichia coli*. *J. Biol. Chem.* 277, 24155–24161. <https://doi.org/10.1074/jbc.M110715200>.
- Kenney, L.J., Anand, G.S., 2020. EnvZ/OmpR two-component signaling: an archetype system that can function noncanonically. *EcoSal* 9, 1–47. <https://doi.org/10.1128/ecosalplus.esp-0001-2019>.
- Payne, R.B., Casalot, L., Rivere, T., Terry, J.H., Larsen, L., Giles, B.J., Wall, J.D., 2004. Interaction between uranium and the cytochrome c3of *Desulfovibrio desulfuricans* strain G20. *Arch. Microbiol.* 181, 398–406. <https://doi.org/10.1007/s00203-004-0671-7>.
- Braeken, K., Moris, M., Daniels, R., Vanderleyden, J., Michiels, J., 2006. New horizons for (p)ppGpp in bacterial and plant physiology. *Trends Microbiol.* 14, 45–54. <https://doi.org/10.1016/j.tim.2005.11.006>.
- Cavalheiro, J.M.B.T., de Almeida, M.C.M.D., Grandfils, C., da Fonseca, M.M.R., 2009. Poly(3-hydroxybutyrate) production by *Cupriavidus necator* using waste glycerol. *Process Biochem.* 44, 509–515. <https://doi.org/10.1016/j.procbio.2009.01.008>.
- Yang, K., Wang, M., Metcalf, W.W., 2009. Uptake of glycerol-2-phosphate via the ugp-encoded transporter in *Escherichia coli* K-12. *J. Bacteriol.* 191, 4667–4670. <https://doi.org/10.1128/JB.00235-09>.
- Orellana, R., Hixson, K.K., Murphy, S., Mester, T., Sharma, M.L., Lipton, M.S., Lovley, D.R., 2014. Proteome of *Geobacter sulfurreducens* in the presence of U(VI). *Microbiol. (U. Kingd.)* 160, 2607–2617. <https://doi.org/10.1099/mic.0.081398-0>.
- Nies, D., Mergeay, M., Friedrich, B., Schlegel, H.G., 1987. Cloning of plasmid genes encoding resistance to cadmium, zinc, and cobalt in *Alcaligenes eutrophus* CH34. *J. Bacteriol.* 169, 4865–4868. <https://doi.org/10.1128/jb.169.10.4865-4868.1987>.
- Nongkhlaw, M., Joshi, S.R., 2019. Molecular insight into the expression of metal transporter genes in *Chryseobacterium* sp. PMSZPI isolated from uranium deposit. *PLoS One* 14, 1–10.
- Monsieurs, P., Moors, H., Van Houdt, R., Janssen, P.J., Janssen, A., Coninx, I., Mergeay, M., Leys, N., 2011. Heavy metal resistance in *Cupriavidus metallidurans* CH34 is governed by an intricate transcriptional network. *BioMetals* 24, 1133–1151. <https://doi.org/10.1007/s10534-011-9473-y>.